

Reduced proteasome activity in the aging brain results in ribosome stoichiometry loss and aggregation

Erika Kelmer Sacramento^{1†}, Joanna M. Kirkpatrick^{1†}, Mariateresa Mazzetto^{1,2†}, Simone Di Sanzo¹, Cinzia Caterino^{1,2}, Michele Sanguanini³, Nikoletta Papaevgeniou⁴, Maria Lefaki⁴, Dorothee Childs⁵, Sara Bagnoli², Eva Terzibasi Tozzini², Aleksandar Bartolome¹, Natalie Romanov⁵, Mario Baumgart¹, Wolfgang Huber⁵, Niki Chondrogianni⁴, Michele Vendruscolo³, Alessandro Cellerino^{1,2*} and Alessandro Ori^{1*#}

Affiliations

¹ Leibniz Institute on Aging – Fritz Lipmann Institute (FLI), Jena, Germany.

² Bio@SNS, Scuola Normale Superiore, Pisa, Italy.

³ Centre for Misfolding Diseases, Department of Chemistry, University of Cambridge, Cambridge, UK.

⁴ Institute of Biology, Medicinal Chemistry and Biotechnology, National Hellenic Research Foundation, Athens, Greece.

⁵ European Molecular Biology Laboratory, Heidelberg, Germany.

*Correspondence to: alessandro.ori@leibniz-fli.de or alessandro.cellerino@sns.it

†These authors contributed equally to this work

Lead contact

Summary

A progressive loss of protein homeostasis is characteristic of aging and a driver of neurodegeneration. To investigate this process quantitatively, we characterized proteome dynamics during brain aging by using the short-lived vertebrate *Nothobranchius furzeri* and combining transcriptomics, proteomics and thermal proteome profiling. We found that the correlation between protein and mRNA levels is progressively reduced during aging, and that post-transcriptional mechanisms are responsible for over 40% of these alterations. These changes induce a progressive stoichiometry loss in protein complexes, including ribosomes, which have low thermal stability in brain lysates and whose component proteins are enriched in aggregates found in old brains. Mechanistically, we show that reduced proteasome activity occurs early during brain aging, and is sufficient to induce loss of stoichiometry. Our work thus defines early events in the aging process that can be targeted to prevent loss of protein homeostasis and age-related neurodegeneration.

Keywords

Aging, brain, protein complex, aggregation, proteome, transcriptome, proteasome, ribosome, stoichiometry

Highlights

- Timeline of proteome changes during killifish brain aging
- Progressive loss of stoichiometry affects multiple protein complexes
- Ribosomes have low thermal stability and aggregate in old brains
- Partial reduction of proteasome activity is sufficient to induce loss of stoichiometry

5

Introduction

Although age is the primary risk factor for cognitive decline and dementia (Assoc, 2018), the associated age-dependent molecular changes are still not known in detail. Despite the presence of clear functional impairments (Buckner, 2004), physiological brain aging is characterized by limited loss of neurons (Schmitz and Hof, 2007) and specific morphological changes of synaptic contacts (Dickstein et al., 2013). Large collections of data for transcript dynamics in human and animal brains indicate that systematic, age-dependent changes in gene expression are also relatively minor (Cellerino and Ori, 2017), although some shared transcriptional signatures have been identified, including a chronic activation of cellular inflammatory response (Aramillo Irizar et al., 2018), reactive changes in glial cells (Clarke et al., 2018) and reduced expression of neuronal and synaptic genes (Lu et al., 2004; Somel et al., 2010).

Since the vast majority of human neurons are generated during fetal and perinatal life and neuronal turnover is limited in the postnatal human brain (Sorrells et al., 2018), neurons are particularly prone to accumulate misfolded proteins that are not properly processed by the cellular proteolytic mechanisms (proteasomal and autophagic pathways), thus forming aberrant deposits. Indeed, neurodegenerative diseases are characterized by the prominent presence of protein aggregates, in particular due to mutations that facilitate misfolding and aggregation, and impairment of cellular quality control systems (Soto and Pritzkow, 2018). Accumulation of protein aggregates occurs also during physiological aging, as demonstrated by the presence of lipofuscin (Glees and Hasan, 1976) and ubiquitinated cellular inclusions (Zeier et al., 2011). Protein aggregation may be related to a decline of proteasome activity, as suggested by the fact that pharmacological inhibition of the proteasome is sufficient to induce intracellular aggregates in young brains (Matsui et al., 2010). However, the exact composition of these spontaneous aggregates and the mechanisms triggering their formation during brain aging remain unknown.

Although age-dependent transcript changes in the brain have been studied extensively (Blalock et al., 2003; Colantuoni et al., 2011; Loerch et al., 2008; Lu et al., 2004; Wood et al., 2013), we are just beginning to understand the corresponding global regulation of the proteome during aging (Ori et al., 2015; Somel et al., 2010; Walther et al., 2015). Substantial post-transcriptional regulation takes place in the aging brain, with a sizeable proportion of proteins being up or downregulated in the absence of changes in the levels of the corresponding transcripts (Ori et al., 2015), resulting in a progressive mRNA-protein decoupling (Janssens et al., 2015; Wei et al., 2015). Protein aggregation and changes in protein stability could play a role in generating an imbalance between protein and transcript levels, but these aspects have not yet been investigated systematically in vertebrate brains.

To address this challenge, we studied the annual killifish *Nothobranchius furzeri*, which is the shortest-lived vertebrate that can currently be bred in captivity. With a lifespan of 3–7

months (Hu and Brunet, 2018; Ripa et al., 2017; Terzibasi et al., 2008; Valdesalici and Cellerino, 2003), it has emerged as a convenient model organism to investigate genetic and non-genetic interventions on aging (Cellerino et al., 2016; Harel et al., 2015; Kim et al., 2016; Platzer and Englert, 2016; Ripa et al., 2017), since it replicates many typical aspects of vertebrate brain aging at the levels of behaviour (Valenzano et al., 2006a; Valenzano et al., 2006b), neuroanatomy (Tozzini et al., 2012) and global gene expression (Aramillo Irizar et al., 2018; Baumgart et al., 2014). Age-dependent processes are enhanced in this species, thus facilitating the detection of differentially expressed genes as compared to other model organisms (Baumgart et al., 2014; Frahm et al., 2017; Wood et al., 2013). For example, an age-dependent formation of inclusion bodies containing α -synuclein and spontaneous degeneration of dopaminergic neurons has been recently described in killifish (Matsui et al., 2019), making it an attractive system to study age-related neurodegenerative disorders and therapeutic strategy against them.

Here, we applied RNAseq, mass spectrometry based proteomics, thermal proteome profiling and analysis of protein aggregates in killifish of different ages to delineate a timeline of molecular events responsible for loss of proteome homeostasis during brain aging. In particular, we set to identify the nature and biophysical properties of proteins that preferentially aggregate in old brains, to comprehensively investigate the loss of stoichiometry of protein complexes and the role played by the proteasome as an early driver of protein homeostasis collapse.

Results and Discussion

Transcript and protein levels become progressively decoupled during brain aging. We analysed whole brains from animals of 3 different age groups by liquid chromatography tandem mass spectrometry using a label-free method (Figure 1A and Table S2). Principal component analysis recovered the three groups (Figure 1B). Higher proteome coverage was obtained by two experiments based on tandem mass tag (TMT) multiplexing, where we compared adult (12 weeks post-hatching, wph) vs. young fish (5 wph) (Figure S1A), and old (39 wph) vs. adult fish, (Figure S1B). A total of 8885 protein groups were quantified with at least two proteotypic peptides, of which 7200 were quantified in both experiments (Figure S1C). Almost one fifth of the quantified protein groups (1720/8885) was affected by aging in at least one of the age comparisons (Table S3). Functionally related proteins showed different patterns of abundance change between age groups, and pathways affected by aging in other species, including inflammation-related pathways (Aramillo Irizar et al., 2018) and the complement and coagulation cascade (Clarke et al., 2018), were retrieved in killifish already in the transition from young to adult (Figure S1D, S1E and Table S3).

Total RNAseq after rRNA depletion and microRNAseq were obtained from the same samples (Table S4). For each sample, absolute protein abundances estimated from peptide intensities (iBAQ values, (Schwanhäusser et al., 2011)) were correlated with the corresponding transcript levels obtained by RNAseq (RPKM values), obtaining global protein-transcript correlation values for each sample separately. We observed a progressive age-dependent reduction of protein-transcript correlation values (Figure 1C), consistent with a decoupling between RNA transcripts and proteins during brain aging (Wei et al., 2015). Decoupling was observed also when analysing an independent RNAseq dataset from polyA+ RNA for animals of the same age groups (Baumgart et al., 2014) (Figure S1F). Fold-changes of genes differentially expressed in the two RNAseq datasets were strongly correlated (Figure S1G). For further

analysis, we then focused on the dataset with higher sequencing depth and larger number of replicates, for which the absolute number of differentially expressed genes was higher (Figure S1H).

5 Direct comparison of protein and mRNA fold changes across age groups (Table S5) revealed discrepancies between RNA and protein regulation (Figure 1D, 1E and Table S1). Protein and transcript changes were significantly correlated in the adult vs. young fish comparison (Figure 1D), but the correlation was reduced in the old vs. adult comparison (Figure 1E), further supporting a progressive decoupling between transcript and protein regulation. For validation, we analyzed proteins previously identified to be very long-lived in rodent brain 10 (Toyama et al., 2013), including histones, collagens and myelin proteins. For these proteins, we found that transcript, but not protein levels, were generally decreased in old fish, indicating that protein stability contributes to the observed discrepancies between transcripts and proteins 15 (Figure S2A). In contrast, immunoreactivity for the glial fibrillary acidic protein (GFAP), but not its RNA levels, were shown to increase significantly in the aging brain (Terzibasi Tozzini et al., 2012), as we confirmed in our data (Figure S2B).

To find out whether microRNAs could contribute to transcript-protein decoupling, we 20 first analysed miRNA expression levels across the same three age groups (Table S4), then mapped the targets of age-affected miRNAs to our proteome data (Figure S2C). By taking into account potential regulation mediated by miRNAs, we defined a subset of proteins whose abundance is affected by aging via mechanisms independent of both transcript level and miRNA-mediated post transcriptional regulation (Figure 1F). This subset accounted for 30% of the affected proteins in the adult vs. young fish comparison, and increased up to 43% in the old vs. adult comparison.

To clarify whether the transcript-protein decoupling preferentially affects some specific 25 pathways, we classified age-affected genes according to their respective transcript and protein fold changes, and performed pathway overrepresentation analysis (Table S5). In the comparison adult vs. young fish, pathways related to the complement coagulation cascade and synaptic function/plasticity were overrepresented in concordantly increased transcript and protein levels, in agreement with the notion that synaptogenesis continues during this phase of residual brain growth (Tozzini et al., 2012). By contrast, genes coding for biosynthetic pathways such as RNA 30 transport, splicing and surveillance of RNA, ribosome biogenesis, and protein processing in the endoplasmic reticulum (ER) were overrepresented in concordantly decreased proteins/transcripts (Figure 1G). These changes may be related to the reduction of adult neurogenesis occurring during this period (Tozzini et al., 2012), and account for a significant fraction of global transcription regulation (Baumgart et al., 2014). The same biosynthetic pathways become discordant when old and adult animals are compared, with protein levels decreasing further with age, while transcript levels changed directionality and increased (Figure 1H, bottom right quadrant).

Taken together, our data indicate that post-transcriptional mechanisms regulating protein 40 levels have an increasingly important role in modulating protein abundance with age; they are responsible for nearly half of the protein changes observed in old brains, and they can lead to the opposite regulation trends for proteins and mRNAs.

5 **Widespread stoichiometric imbalance in protein complexes during aging.** Amongst genes showing opposite transcript and protein changes already in the adult vs. young fish comparison, we identified 13 genes encoding ribosomal proteins with transcript levels being significantly increased and protein abundances decreased (Figure 2A and Figure S3A). Fold changes of genes encoding for ribosomal proteins split into two groups in the old vs. adult fish comparison (Figure 1H): while transcript levels increase in a concordant way, similarly to the adult vs. young fish comparison, ribosomal proteins show either increased (13 proteins, e.g., RPS20, RPL8 and RPL21) or decreased (14 proteins, e.g., RPS6, RPLP2 and RPL22L1) abundance (Figure 2A and S3A). These findings indicate a loss of stoichiometry (i.e. an imbalance in their relative levels) of 10 ribosomal proteins during aging, which is likely to impair ribosome assembly and to create a pool of orphan proteins at risk of aggregation. When mapped on the ribosome structure (Khatter et al., 2015), age-affected proteins form clusters of either consistently increased or decreased abundance (Figure 2B). Since transcript level changes are consistent, while ribosomal protein levels are not (Figure S3A), the loss of ribosome stoichiometry must result from an alteration of 15 post-transcriptional mechanisms mediating protein homeostasis.

20 We next asked whether the age-related loss of stoichiometry described above occurs more widely in the proteome. We thus analysed all annotated protein complexes in the two age group comparisons (Ori et al., 2013; Ori et al., 2016). We found that the number of complexes undergoing stoichiometry changes increases from 11% (16 out of 140) between 5 and 12 wph, to 25 30% (39 out of 129) between 12 and 39 wph (Figure 2C and Table S6). Consistently, the number of affected complex members increases almost 2-fold in the old vs. adult comparison (from 7% to 13%) (Figure S3B). Loss of stoichiometry was confirmed by an alternative metric, namely an increase in the inter-quantile range (IQR) of fold changes of protein complex members (Janssens et al., 2015) in the old vs. adult fish comparison. By contrast, the IQRs of transcripts coding for the same complex members were decreased (Figure 2D), demonstrating that post-transcriptional mechanisms are responsible for the age-related global loss of stoichiometry in protein complexes.

30 When individual complexes were ranked according to the difference of IQR between the two age comparisons, the majority of the complexes showed an increase in IQR (76 out of 124, 61%, Figure 2E and Table S6). The most affected complexes included Complex IV and Complex 35 V of the mitochondrial respiratory chain, but not Complex I and Complex III, the cytoplasmic ribosome, the 26S proteasome, the B complex of the spliceosome, and the lysosomal V-type ATPase (Figure 2E and 2F). These complexes take part in biological processes known to be causative in aging (Carmona-Gutierrez et al., 2016; Chondrogianni et al., 2014; Dillin et al., 2002; Heintz et al., 2017; Lee et al., 2003; Steffen and Dillin, 2016), and the expression of transcripts coding for them were previously shown to be correlated with individual lifespan in a longitudinal RNAseq study in *N. furzeri* (Baumgart et al., 2016). Many of these complexes are affected by stoichiometry changes already at the adult stage (Table S6), identifying these alterations as early events during aging progression.

40

45 **Thermal proteome profiling reveals minor changes of protein thermal stability with aging.** A major question arising from our findings is whether the stoichiometric changes described here influence complex stability or other features. To answer this question, we globally evaluated protein stability in young and old brain lysates using thermal proteome profiling (TPP) (Becher et al., 2018; Savitski et al., 2014; Tan et al., 2018) (Figure 3A). We measured melting

temperature (T_m) for 2287 protein groups in four independent pools of brains obtained from young and old killifish (Table S7). The T_m values obtained in the two biological replicates were strongly correlated (Figure S4A).

We next related the experimentally derived T_m values to biophysical properties known to influence protein folding. We found that the predicted molecular chaperone requirement for folding is correlated with thermal stability in brain lysates; in particular, proteins that do not depend on molecular chaperones to fold show a statistically significant increased average T_m both in young and old animals (Figure 3B). A similar correlation was previously observed for Hsp90 clients in intact cells (Savitski et al., 2018), thus supporting the validity of our approach in whole brains.

Next, we performed an analysis to identify gene sets enriched among low- or high-thermally stable proteins. To increase the number of analysed proteins, ranking was based on the area under the curve (AUC) obtained from the melting curve of each individual protein (Childs et al., 2018). We could rank 6337 protein groups. The ribosome, t-RNA biosynthesis, and pathways related to synaptic plasticity (e.g., “Long-term depression” and “Long term potentiation”) were significantly enriched among the less thermally stable proteins, and proteins of higher thermal stability were enriched for lysosomal and SNARE proteins (Figure 3C and Table S7). We found that ribosomes and the 26S proteasome are among the least thermally stable complexes (Figure 3D). We observed that median T_m values of protein complexes were highly correlated between young and old animals with the exception of the lysosomal vATPase, which showed higher thermal stability in old killifish brain (Figure 3E).

We also globally assessed age-related changes of thermal stability for individual proteins. The distribution of AUC differences between young and old samples was symmetric around zero (Figure 3F), indicating that aging does not cause a global reduction of protein thermal stability. We identified 47 proteins significantly affected (Figure S4B and Table S7). Among the top hits, we found increased stability of the mTOR Complex 1 (mTORC1) regulator RRAGA, which is also known to have a direct interaction with the lysosomal vATPase (Zoncu et al., 2011) (Figure 3G). Taken together, our data show that the thermal stability of few proteins is affected by aging and that there are no major changes in the stability of protein complexes, despite alteration of their stoichiometry, with the possible exception of vATPase and its interactors, indicating that once formed, protein complexes tend to be similarly stable at all ages.

Age-dependent protein aggregates are enriched for ribosomal proteins. Although the stoichiometry loss in protein complexes does not destabilise the complexes themselves, as we noted above, it can still create a pool of orphan proteins at risk of aggregation. Since protein aggregates are known to be SDS-insoluble (Reis-Rodrigues et al., 2012), we compared SDS-insoluble fractions from brain homogenates of young and old animals (Figure 4A and Figure S5A). We used mice for this analysis because of the larger brain size that allows retrieval of sufficient amount of aggregates for proteomic analysis. As expected, the yield of SDS-insoluble protein aggregates was significantly higher from old animals, confirming that aging is associated with enhanced protein aggregation (Figure 4B and Figure S5B). We then analysed the aggregate composition by quantitative mass spectrometry to identify proteins enriched in these aggregates as compared to the starting total brain homogenates. We quantified 965 protein groups across three independent experiments, and identified 56 significantly enriched proteins (Table S8).

Enriched proteins showed a predicted higher molecular chaperone requirement for folding, and were richer in intrinsically disordered regions (Figure 4C). Among the enriched proteins, we found collagens (Col1a1, Col1a2 and Col4a2), which are well-known to undergo age-dependent crosslinking (Viidik, 1979), and ferritins (Fth1 and Ftl1), whose aggregation is linked to the age-dependent brain accumulation of intracellular iron (Ripa et al., 2016; Zecca et al., 2004) (Figure 4D). Protein aggregates were also enriched for ribosomal proteins (Figure 4D and S5D) that are both characterised by protein transcript decoupling (Figure 1H) and loss of complex stoichiometry (Figure 2A and 2B) during aging. Other protein complexes that displayed loss of stoichiometry (i.e., Complex V and vATPase) did not show significant enrichment in aggregates, indicating that stoichiometry imbalances do not always correlate with protein aggregation (Figure S5D).

To confirm the aggregation of ribosomal proteins in killifish, we performed staining of young (7-10 wph) and old (27-30 wph) brain slices using Proteostat, an amyloid-specific dye (Shen et al., 2011). As expected, we detected lysosomal aggregates in old but not in young brains (Figure S5E, S5F and S5H). These aggregates appeared to contain the ribosomal protein RPS6 (Figure 4E and S5G). Taken together, these data demonstrate that an age-dependent aggregation of ribosomal proteins is conserved in both old fish and old mice.

Reduced proteasome activity contributes to loss of protein stoichiometry in primary human fibroblasts. Since protein stoichiometry loss could be due to decreased proteolysis rates, we focused on the proteasome, which is one of the main degradation machineries and itself undergoes stoichiometry loss upon aging (Figure 2E). First, we observed a decrease in the levels of both proteasome proteins and their transcripts in adult killifish, which was followed by a stoichiometry imbalance that manifested in old fish exclusively at the protein level. In particular, we observed an imbalance between proteins belonging to the 19S and the 20S complexes, with the latter being exclusively upregulated in old fish (Figure 5A and 5B).

To further investigate the proteasome functional status in killifish brains of different age groups, we performed native gel electrophoresis of proteasomes accompanied by in-gel proteasome activity assays (Chondrogianni et al., 2015). A significant decrease in the levels of both 30S (double-capped) and 26S (single-capped) proteasomes was revealed already in adult animals (Figure 5C and S6A). This decrease was accompanied by a significant reduction of all three proteasome activities in adult and old samples compared to young samples (Figure 5D and S6B).

To assess whether this decline is relevant for lifespan determination, we re-analyzed a longitudinal study of RNAseq, where transcripts from fin biopsies were quantified at 10 and 20 wph, and variations in gene expression were correlated with individual variations in lifespan (Baumgart et al., 2016). We observed that the shortest-lived individuals of the cohort were characterized by a larger age-dependent downregulation of transcripts coding for proteasomal proteins, which was absent in the longest-lived individuals (Figure 5E), indicating that the rate of proteasome downregulation in early adult life is predictive of lifespan in killifish.

We then asked whether reduced proteasome function can induce stoichiometry loss of protein complexes. To answer this question, we used HFL-1 human primary lung fibroblasts as a model system for the following reasons: (i) these cells are a standard *in vitro* model for aging studies because they undergo replicative senescence (Hayflick, 1965), and (ii) senescent

fibroblasts have been shown to possess reduced proteasome activities (Chondrogianni et al., 2003). We treated young fibroblasts with epoxomicin, a selective and irreversible proteasome inhibitor, for 4 days at a dosage that induces 50% reduction of proteasome activity, resembling the reduction of activity exhibited by senescent HFL-1 fibroblasts (Chondrogianni et al., 2003).

5 We then analysed proteome changes in epoxomicin- vs. vehicle control-treated HFL-1 cells, and compared it to changes induced by replicative senescence. In order to take into account technical and biological variability, we included an additional comparison of non-senescent cells at different passages (Figure 6A and Table S9). Principal component analysis on protein abundance profiles revealed that samples cluster according to their condition (Figure S7A). Increased protein levels GLB1, the enzyme responsible for the senescence associated beta-galactosidase activity (Lee et al., 2006), confirmed the senescent phenotype of old fibroblasts (Figure S7B).

10 Increased levels of proteasome subunits, a known compensatory reaction to proteasome inhibition (Li et al., 2011; Wojcik and DeMartino, 2002), were detected in epoxomicin-treated cells (Figure S7C). In both epoxomicin-treated cells and senescent fibroblasts, we detected changes in protein complex stoichiometries (Figure S7D and S7E) and a global increase of IQRs for members of protein complexes (Figure 6B), resembling the aging phenotype observed in killifish brain (Figure 2C and 2D). Proteasome inhibition and replicative senescence both led to decreased levels of ribosomal proteins (Figure S7F) that affected most, but not all, the components of the ribosome (Figure S7G). As a consequence, we observed a significant increase in the IQRs of both small and large subunits of the ribosome (Figure 6C), indicating loss of ribosome stoichiometry. Taken together, these data demonstrate that a partial reduction of proteasome activity occurs in killifish brain starting from adult age, and that inducing a comparable reduction of proteasome activity in primary human fibroblast is sufficient to induce a loss of protein complex stoichiometry that is also observable in senescent cells.

25

A molecular timeline for aging. Our results delineate a timeline of events associated with loss of protein quality control upon aging. An early event, detectable already in adult fish, is a decreased proteolytic activity of the proteasome, which is driven by a downregulation of transcripts coding for components of the 19S and 20S complexes in adult fish brain (Figure 5A and 5B). The amplitude of this downregulation correlated with individual lifespan and could represent an early biomarker of aging (Figure 5E). The reduction of proteasome activity precedes chronologically the decoupling of transcript/protein levels, suggesting a causative role in this aspect of the aging process. Decreased proteasome activity can lead to the accumulation of proteins that are synthesized in excess relative to their binding partners, thus causing a stoichiometric imbalance of protein complexes (McShane et al., 2016). For instance, deletion of the ubiquitin ligase Tom1 (yeast homologue of Huwe1), which is responsible for the labelling for degradation of overproduced ribosomal proteins, leads to accumulation of multiple ribosomal proteins in detergent-insoluble aggregates in yeast (Sung et al., 2016). Accumulation of ribosomes in detergent-insoluble aggregates (David et al., 2010) and a loss of stoichiometry in the proteasome (Walther et al., 2015) were previously reported to occur during aging in *C. elegans*. Our work demonstrates the conservation of these mechanisms in the vertebrate brain, by showing alteration of stoichiometry in several large protein complexes (Figure 2C and 2D) and aggregation of ribosomes in old brain (Figure 4D and 4E). Specifically, we establish a mechanistic link between the partial reduction of proteasome activity observed in adult brains and the loss of stoichiometry of protein complexes (Figure 6B and 6C).

Later in life, the stoichiometry imbalance in protein complexes contributes to exacerbate the loss of protein homeostasis. Proteasome activity is further reduced in the old brain, correlating with an increased imbalance between the 19S and 20S complexes with time (Figure 5B and 5C). In addition, altered stoichiometry of the ribosome can underlie both the reduction and the qualitative changes of protein synthesis in brain aging (Ori et al., 2015; Schimanski and Barnes, 2010; Sudmant et al., 2018). An alteration of the stoichiometry between membrane-bound and cytosolic components of the lysosomal v-type ATPase (Figure 2F) might influence the acidification of lysosomes and the activation of mTORC1 (Zoncu et al., 2011), thus hampering the clearance of protein aggregates. These aggregates in turn may further impair the proteasome activity (Grune et al., 2004), thus creating a negative feedback loop. Other key pathways implicated in aging are affected by this loss of stoichiometry: in particular, alterations of respiratory chain complexes (particularly Complex IV and V) might contribute to their decreased activity and increased ROS production in old brain (Stefanatos and Sanz, 2018), and changes in multiple spliceosome complexes might underlie previously observed qualitative changes of splicing (Ori et al., 2015). More detailed mechanistic studies are needed to demonstrate that the alterations that we have described are sufficient to impair the function of these protein complexes during aging.

It remains to be determined which mechanisms promote the early decrease of proteasome activity already in adult fish. Our data point to multiple processes being involved, including in particular: (i) decreased levels of rate-limiting proteasome members for the production of 20S assembled/functional proteasomes (e.g., PSMB5 or PSMB6, (Chondrogianni et al., 2015)), which we found to be significantly decreased already in the adult fish (Figure 5B); (ii) changes in abundance of proteasome proteins that are important for the assembly and activity of the 19S proteasome complex, such as PSMD8. PSMD8 was shown to bridge the lid and the base of the 19S complex and to mediate the lid-base joining, thus being a crucial factor for the assembly of the 30S/26S proteasome (Tomko and Hochstrasser, 2011). We found that PSMD8 is destabilized in old killifish (Figure S4B), suggesting a change in its assembly status that could explain the loss of 30S/26S complexes observed in the adult and old fish (Figure 5C). PSMD5 has been also shown to inhibit the assembly and activity of the 26S proteasome, and this proteasome member has been shown to be induced by inflammation (Shim et al., 2012). Accordingly, we detected also in killifish an activation of inflammation-related pathways (Figure S1D and S1E) and, importantly, we identified PSMD5 as one of the few proteasome members to be upregulated in the adult fish (Figure 5B). Finally, PSMD11 (known as RPN-6 in *C. elegans*), which has been shown to be responsible for increased proteasome assembly and activity in human embryonic stem cells and in *C. elegans* (Vilchez et al., 2012), was significantly downregulated already in adult fish (Figure 5B). Identifying ways of counteracting these mechanisms might provide new avenues to delay organ dysfunction in aging and to increase lifespan. In this context, multiple studies have reported that transgenic animals (from various species) engineered to have enhanced proteasome activity show increased health- and lifespan (Augustin et al., 2018; Chondrogianni et al., 2015; Vilchez et al., 2012), and correspondingly we have shown that expression level of proteasome genes predicts life expectancy in killifish (Figure 5E).

In conclusion, our work identifies the maintenance of proteasome activity upon aging as being critical to ensure the correct stoichiometry of protein complexes, thus preserving key biological functions, primarily protein synthesis, degradation, and energy production.

Acknowledgments: The authors gratefully acknowledge support from the FLI Core Facilities Proteomics, Sequencing, and Bioinformatics, and the Fish Facility. The authors would like to acknowledge Stephan Schacke for assistance in data visualization, Toby Mathieson and Holger Dinkel for assistance in establishing data analysis pipelines, and Martin Beck, K. Lenhard Rudolph, David M. Sabatini, Maria Ermolaeva, Monther Abu-Ramaileh and Aliaksandr Khaminets for critical comments on the manuscript and helpful discussions. The FLI is a member of the Leibniz Association and is financially supported by the Federal Government of Germany and the State of Thuringia. AO and SDS acknowledge funding from the German Research Council (Deutsche Forschungsgemeinschaft, DFG) via the Research Training Group ProMoAge (GRK 2155). Research from NC lab is currently co-financed by the European Union and Greek national funds through the Operational Program Competitiveness, Entrepreneurship and Innovation under the call RESEARCH – CREATE – INNOVATE (project codes: T1EDK-00353 and T1EDK-01610) and under the Action “Action for the Strategic Development on the Research and Technological Sector” (project STHENOS-b, MIS 5002398). NP receives a PhD fellowship from Empirikon Foundation.

Author contributions: Conceptualization: EKS, JMK, MM, NC, MV, AC, AO. Data curation: EKS, JMK, MM, AO. Formal analysis: EKS, JMK, MM, DC, MS, NR, MB, NC, AO. Investigation: EKS, JMK, SDS, CC, NP, ML, ETT, NC. Methodology: EKS, JMK, MM, DC. Project administration: AC, AO. Resources: MB. Data analysis: MM, MS, DC, NR, WH, AO. Supervision: JMK, WH, NC, MV, AC, AO. Visualization: EKS, JMK, MM, SDS, MS, DC, SB, ETT, AB, AO. Writing – original draft: EKS, JMK, MM, MV, AC, AO. Writing – review & editing: MS, ETT, NR, NC.

Declaration of interests: Authors declare no competing interests.

References

- Aramillo Irizar, P., Schable, S., Esser, D., Groth, M., Frahm, C., Priebe, S., Baumgart, M., Hartmann, N., Marthandan, S., Menzel, U., *et al.* (2018). Transcriptomic alterations during ageing reflect the shift from cancer to degenerative diseases in the elderly. *Nature communications* *9*, 327.
- Assoc, A.s. (2018). 2018 Alzheimer's disease facts and figures. *Alzheimers Dement* *14*, 367-425.
- Augustin, H., McGourty, K., Allen, M.J., Adcott, J., Wong, C.T., Boucrot, E., and Partridge, L. (2018). Impact of insulin signaling and proteasomal activity on physiological output of a neuronal circuit in aging *Drosophila melanogaster*. *Neurobiology of aging* *66*, 149-157.
- Baumgart, M., Groth, M., Priebe, S., Savino, A., Testa, G., Dix, A., Ripa, R., Spallotta, F., Gaetano, C., Ori, M., *et al.* (2014). RNA-seq of the aging brain in the short-lived fish *N. furzeri* - conserved pathways and novel genes associated with neurogenesis. *Aging cell*.
- Baumgart, M., Priebe, S., Groth, M., Hartmann, N., Menzel, U., Pandolfini, L., Koch, P., Felder, M., Ristow, M., Englert, C., *et al.* (2016). Longitudinal RNA-Seq Analysis of Vertebrate Aging Identifies Mitochondrial Complex I as a Small-Molecule-Sensitive Modifier of Lifespan. *Cell Syst* *2*, 122-132.
- Becher, I., Andres-Pons, A., Romanov, N., Stein, F., Schramm, M., Baudin, F., Helm, D., Kurzawa, N., Mateus, A., Mackmull, M.T., *et al.* (2018). Pervasive Protein Thermal Stability Variation during the Cell Cycle. *Cell* *173*, 1495-1507 e1418.
- Blalock, E.M., Chen, K.C., Sharro, K., Herman, J.P., Porter, N.M., Foster, T.C., and Landfield, P.W. (2003). Gene microarrays in hippocampal aging: statistical profiling identifies novel processes correlated with cognitive impairment. *J Neurosci* *23*, 3807-3819.
- Buckner, R.L. (2004). Memory and executive function in aging and AD: multiple factors that cause decline and reserve factors that compensate. *Neuron* *44*, 195-208.
- Carmona-Gutierrez, D., Hughes, A.L., Madeo, F., and Ruckenstuhl, C. (2016). The crucial impact of lysosomes in aging and longevity. *Ageing Res Rev* *32*, 2-12.
- Cellerino, A., and Ori, A. (2017). What have we learned on aging from omics studies? *Seminars in cell & developmental biology* *70*, 177-189.
- Cellerino, A., Valenzano, D.R., and Reichard, M. (2016). From the bush to the bench: the annual *Nothobranchius* fishes as a new model system in biology. *Biological reviews of the Cambridge Philosophical Society* *91*, 511-533.
- Childs, D., Bach, K., Franken, H., Anders, S., Kurzawa, N., Bantscheff, M., Mikhail, S., and Huber, W. (2018). Non-Parametric Analysis of Thermal Proteome Profiles Reveals Novel Drug-Binding Proteins. *bioRxiv*.
- Chondrogianni, N., Georgila, K., Kourtis, N., Tavernarakis, N., and Gonos, E.S. (2015). 20S proteasome activation promotes life span extension and resistance to proteotoxicity in *Caenorhabditis elegans*. *FASEB J* *29*, 611-622.
- Chondrogianni, N., Sakellari, M., Lefaki, M., Papaevgeniou, N., and Gonos, E.S. (2014). Proteasome activation delays aging in vitro and in vivo. *Free Radic Biol Med* *71*, 303-320.
- Chondrogianni, N., Stratford, F.L., Trougakos, I.P., Friguet, B., Rivett, A.J., and Gonos, E.S. (2003). Central role of the proteasome in senescence and survival of human fibroblasts: induction of a senescence-like phenotype upon its inhibition and resistance to stress upon its activation. *J Biol Chem* *278*, 28026-28037.

- Clarke, L.E., Liddelow, S.A., Chakraborty, C., Munch, A.E., Heiman, M., and Barres, B.A. (2018). Normal aging induces A1-like astrocyte reactivity. *Proceedings of the National Academy of Sciences of the United States of America* *115*, E1896-E1905.
- 5 Colantuoni, C., Lipska, B.K., Ye, T., Hyde, T.M., Tao, R., Leek, J.T., Colantuoni, E.A., Elkahloun, A.G., Herman, M.M., Weinberger, D.R., *et al.* (2011). Temporal dynamics and genetic control of transcription in the human prefrontal cortex. *Nature* *478*, 519-523.
- David, D.C., Ollikainen, N., Trinidad, J.C., Cary, M.P., Burlingame, A.L., and Kenyon, C. (2010). Widespread protein aggregation as an inherent part of aging in *C. elegans*. *PLoS Biol* *8*, e1000450.
- 10 Dickstein, D.L., Weaver, C.M., Luebke, J.I., and Hof, P.R. (2013). Dendritic spine changes associated with normal aging. *Neuroscience* *251*, 21-32.
- Dillin, A., Hsu, A.L., Arantes-Oliveira, N., Lehrer-Graiwer, J., Hsin, H., Fraser, A.G., Kamath, R.S., Ahringer, J., and Kenyon, C. (2002). Rates of behavior and aging specified by mitochondrial function during development. *Science* *298*, 2398-2401.
- 15 Frahm, C., Srivastava, A., Schmidt, S., Mueller, J., Groth, M., Guenther, M., Ji, Y., Priebe, S., Platzer, M., and Witte, O.W. (2017). Transcriptional profiling reveals protective mechanisms in brains of long-lived mice. *Neurobiology of aging* *52*, 23-31.
- Glees, P., and Hasan, M. (1976). Lipofuscin in neuronal aging and diseases. *Norm Pathol Anat (Stuttg)* *32*, 1-68.
- 20 Grune, T., Jung, T., Merker, K., and Davies, K.J. (2004). Decreased proteolysis caused by protein aggregates, inclusion bodies, plaques, lipofuscin, ceroid, and 'aggresomes' during oxidative stress, aging, and disease. *Int J Biochem Cell Biol* *36*, 2519-2530.
- 25 Harel, I., Benayoun, B.A., Machado, B.E., Priya Singh, P., Hu, C.-K., Pech, M.F., Valenzano, D.R., Zhang, E., Sharp, S.C., Artandi, S.E., *et al.* (2015). A platform for rapid exploration of aging and diseases in a naturally short-lived vertebrate. *Cell*, in press.
- Hayflick, L. (1965). The Limited in Vitro Lifetime of Human Diploid Cell Strains. *Exp Cell Res* *37*, 614-636.
- Heintz, C., Doktor, T.K., Lanjuin, A., Escoubas, C.C., Zhang, Y., Weir, H.J., Dutta, S., Silva-Garcia, C.G., Bruun, G.H., Morantte, I., *et al.* (2017). Splicing factor 1 modulates dietary restriction and TORC1 pathway longevity in *C. elegans*. *Nature* *541*, 102-106.
- 30 Hu, C.K., and Brunet, A. (2018). The African turquoise killifish: A research organism to study vertebrate aging and diapause. *Aging cell* *17*, e12757.
- Janssens, G.E., Meinema, A.C., Gonzalez, J., Wolters, J.C., Schmidt, A., Guryev, V., Bischoff, R., Wit, E.C., Veenhoff, L.M., and Heinemann, M. (2015). Protein biogenesis machinery is a driver of replicative aging in yeast. *eLife* *4*.
- 35 Khatter, H., Myasnikov, A.G., Natchiar, S.K., and Klaholz, B.P. (2015). Structure of the human 80S ribosome. *Nature* *520*, 640-645.
- Kim, Y., Nam, H.G., and Valenzano, D.R. (2016). The short-lived African turquoise killifish: an emerging experimental model for ageing. *Disease models & mechanisms* *9*, 115-129.
- 40 Lee, B.Y., Han, J.A., Im, J.S., Morrone, A., Johung, K., Goodwin, E.C., Kleijer, W.J., DiMaio, D., and Hwang, E.S. (2006). Senescence-associated beta-galactosidase is lysosomal beta-galactosidase. *Aging cell* *5*, 187-195.

- Lee, S.S., Lee, R.Y., Fraser, A.G., Kamath, R.S., Ahringer, J., and Ruvkun, G. (2003). A systematic RNAi screen identifies a critical role for mitochondria in *C. elegans* longevity. *Nat Genet* 33, 40-48.
- 5 Li, X., Matilainen, O., Jin, C., Glover-Cutter, K.M., Holmberg, C.I., and Blackwell, T.K. (2011). Specific SKN-1/Nrf stress responses to perturbations in translation elongation and proteasome activity. *PLoS Genet* 7, e1002119.
- Loerch, P.M., Lu, T., Dakin, K.A., Vann, J.M., Isaacs, A., Geula, C., Wang, J., Pan, Y., Gabuzda, D.H., Li, C., *et al.* (2008). Evolution of the aging brain transcriptome and synaptic regulation. *PloS one* 3, e3329.
- 10 Lu, T., Pan, Y., Kao, S.Y., Li, C., Kohane, I., Chan, J., and Yankner, B.A. (2004). Gene regulation and DNA damage in the ageing human brain. *Nature* 429, 883-891.
- Matsui, H., Ito, H., Taniguchi, Y., Inoue, H., Takeda, S., and Takahashi, R. (2010). Proteasome inhibition in medaka brain induces the features of Parkinson's disease. *J Neurochem* 115, 178-187.
- 15 Matsui, H., Kenmochi, N., and Namikawa, K. (2019). Age- and α -Synuclein-Dependent Degeneration of Dopamine and Noradrenaline Neurons in the Annual Killifish *Nothobranchius furzeri*. *Cell Reports* 26, 1727-1733.e1726.
- 20 McShane, E., Sin, C., Zauber, H., Wells, J.N., Donnelly, N., Wang, X., Hou, J., Chen, W., Storchova, Z., Marsh, J.A., *et al.* (2016). Kinetic Analysis of Protein Stability Reveals Age-Dependent Degradation. *Cell* 167, 803-815.e821.
- Ori, A., Banterle, N., Iskar, M., Andrés-Pons, A., Escher, C., Khanh Bui, H., Sparks, L., Solis-Mezarino, V., Rinner, O., Bork, P., *et al.* (2013). Cell type-specific nuclear pores: a case in point for context-dependent stoichiometry of molecular machines. *Molecular systems biology* 9, 648.
- 25 Ori, A., Iskar, M., Buczak, K., Kastritis, P., Parca, L., Andrés-Pons, A., Singer, S., Bork, P., and Beck, M. (2016). Spatiotemporal variation of mammalian protein complex stoichiometries. *Genome biology* 17, 47.
- Ori, A., Toyama, B.H., Harris, M.S., Bock, T., Iskar, M., Bork, P., Ingolia, N.T., Hetzer, M.W., and Beck, M. (2015). Integrated Transcriptome and Proteome Analyses Reveal Organ-Specific Proteome Deterioration in Old Rats. *Cell Systems* 1, 224-237.
- 30 Platzer, M., and Englert, C. (2016). *Nothobranchius furzeri*: A Model for Aging Research and More. *Trends in genetics : TIG* 32, 543-552.
- Reis-Rodrigues, P., Czerwieniec, G., Peters, T.W., Evani, U.S., Alavez, S., Gaman, E.A., Vantipalli, M., Mooney, S.D., Gibson, B.W., Lithgow, G.J., *et al.* (2012). Proteomic analysis of age-dependent changes in protein solubility identifies genes that modulate lifespan. *Aging cell* 11, 120-127.
- 35 Ripa, R., Dolfi, L., Terrigno, M., Pandolfini, L., Arcucci, V., Groth, M., Terzibasi Tozzini, E., Baumgart, M., and Cellerino, A. (2016). MicroRNA miR-29 controls a compensatory response to limit neuronal iron accumulation during adult life and aging. *BioRXiv*, <http://dx.doi.org/10.1101/046516>.
- 40 Ripa, R., Dolfi, L., Terrigno, M., Pandolfini, L., Savino, A., Arcucci, V., Groth, M., Terzibasi Tozzini, E., Baumgart, M., and Cellerino, A. (2017). MicroRNA miR-29 controls a compensatory response to limit neuronal iron accumulation during adult life and aging. *BMC Biol* 15, 9.

- Savitski, M.M., Reinhard, F.B.M., Franken, H., Werner, T., Savitski, M.F., Eberhard, D., Molina, D.M., Jafari, R., Dovega, R.B., Klaeger, S., *et al.* (2014). Tracking cancer drugs in living cells by thermal profiling of the proteome. *Science* *346*, 1255784-1255784.
- 5 Savitski, M.M., Zinn, N., Faelth-Savitski, M., Poeckel, D., Gade, S., Becher, I., Muelbaier, M., Wagner, A.J., Strohmer, K., Werner, T., *et al.* (2018). Multiplexed Proteome Dynamics Profiling Reveals Mechanisms Controlling Protein Homeostasis. *Cell* *173*, 260-274 e225.
- Schimanski, L.A., and Barnes, C.A. (2010). Neural Protein Synthesis during Aging: Effects on Plasticity and Memory. *Front Aging Neurosci* *2*.
- 10 Schmitz, C., and Hof, P.R. (2007). Design-Based Stereology in Brain Aging Research. In *Brain Aging: Models, Methods, and Mechanisms*, D.R. Riddle, ed. (Boca Raton (FL)).
- Schwanhäusser, B., Busse, D., Li, N., Dittmar, G., Schuchhardt, J., Wolf, J., Chen, W., and Selbach, M. (2011). Global quantification of mammalian gene expression control. *Nature* *473*, 337-342.
- 15 Shen, D., Coleman, J., Chan, E., Nicholson, T.P., Dai, L., Sheppard, P.W., and Patton, W.F. (2011). Novel cell- and tissue-based assays for detecting misfolded and aggregated protein accumulation within aggresomes and inclusion bodies. *Cell Biochem Biophys* *60*, 173-185.
- Shim, S.M., Lee, W.J., Kim, Y., Chang, J.W., Song, S., and Jung, Y.K. (2012). Role of S5b/PSMD5 in proteasome inhibition caused by TNF-alpha/NFKappaB in higher eukaryotes. *Cell Rep* *2*, 603-615.
- 20 Somel, M., Guo, S., Fu, N., Yan, Z., Hu, H.Y., Xu, Y., Yuan, Y., Ning, Z., Hu, Y., Menzel, C., *et al.* (2010). MicroRNA, mRNA, and protein expression link development and aging in human and macaque brain. *Genome Res* *20*, 1207-1218.
- 25 Sorrells, S.F., Paredes, M.F., Cebrian-Silla, A., Sandoval, K., Qi, D., Kelley, K.W., James, D., Mayer, S., Chang, J., Auguste, K.I., *et al.* (2018). Human hippocampal neurogenesis drops sharply in children to undetectable levels in adults. *Nature* *555*, 377-381.
- Soto, C., and Pritzkow, S. (2018). Protein misfolding, aggregation, and conformational strains in neurodegenerative diseases. *Nat Neurosci* *21*, 1332-1340.
- 30 Stefanatos, R., and Sanz, A. (2018). The role of mitochondrial ROS in the aging brain. *FEBS Lett* *592*, 743-758.
- Steffen, K.K., and Dillin, A. (2016). A Ribosomal Perspective on Proteostasis and Aging. *Cell Metab* *23*, 1004-1012.
- 35 Sudmant, P.H., Lee, H., Dominguez, D., Heiman, M., and Burge, C.B. (2018). Widespread Accumulation of Ribosome-Associated Isolated 3' UTRs in Neuronal Cell Populations of the Aging Brain. *Cell Rep* *25*, 2447-2456 e2444.
- Sung, M.K., Porras-Yakushi, T.R., Reitsma, J.M., Huber, F.M., Sweredoski, M.J., Hoelz, A., Hess, S., and Deshaies, R.J. (2016). A conserved quality-control pathway that mediates degradation of unassembled ribosomal proteins. *eLife* *5*.
- 40 Tan, C.S.H., Go, K.D., Bisteau, X., Dai, L., Yong, C.H., Prabhu, N., Ozturk, M.B., Lim, Y.T., Sreekumar, L., Lengqvist, J., *et al.* (2018). Thermal proximity coaggregation for system-wide profiling of protein complex dynamics in cells. *Science* *359*, 1170-1177.
- Terzibasi, E., Valenzano, D.R., Benedetti, M., Roncaglia, P., Cattaneo, A., Domenici, L., and Cellerino, A. (2008). Large differences in aging phenotype between strains of the short-lived annual fish *Nothobranchius furzeri*. *PloS one* *3*, e3866.

- Terzibasi Tozzini, E., Baumgart, M., Battistoni, G., and Cellerino, A. (2012). Adult neurogenesis in the short-lived teleost *Nothobranchius furzeri*: localization of neurogenic niches, molecular characterization and effects of aging. *Aging cell* 11, 241-251.
- 5 Tomko, R.J., Jr., and Hochstrasser, M. (2011). Incorporation of the Rpn12 subunit couples completion of proteasome regulatory particle lid assembly to lid-base joining. *Mol Cell* 44, 907-917.
- Toyama, B.H., Savas, J.N., Park, S.K., Harris, M.S., Ingolia, N.T., Yates, J.R., and Hetzer, M.W. (2013). Identification of long-lived proteins reveals exceptional stability of essential cellular structures. *Cell* 154, 971-982.
- 10 Tozzini, E.T., Baumgart, M., Battistoni, G., and Cellerino, A. (2012). Adult neurogenesis in the short-lived teleost *Nothobranchius furzeri*: localization of neurogenic niches, molecular characterization and effects of aging. *Aging cell* 11, 241-251.
- Valdesalici, S., and Cellerino, A. (2003). Extremely short lifespan in the annual fish *Nothobranchius furzeri*. *Proc R Soc Lond B Biol Sci* 270 Suppl 2, S189-191.
- 15 Valenzano, D.R., Terzibasi, E., Cattaneo, A., Domenici, L., and Cellerino, A. (2006a). Temperature affects longevity and age-related locomotor and cognitive decay in the short-lived fish *Nothobranchius furzeri*. *Aging cell* 5, 275-278.
- 20 Valenzano, D.R., Terzibasi, E., Genade, T., Cattaneo, A., Domenici, L., and Cellerino, A. (2006b). Resveratrol prolongs lifespan and retards the onset of age-related markers in a short-lived vertebrate. *Curr Biol* 16, 296-300.
- Viidik, A. (1979). Connective tissues--possible implications of the temporal changes for the aging process. *Mech Ageing Dev* 9, 267-285.
- 25 Vilchez, D., Morante, I., Liu, Z., Douglas, P.M., Merkwirth, C., Rodrigues, A.P., Manning, G., and Dillin, A. (2012). RPN-6 determines *C. elegans* longevity under proteotoxic stress conditions. *Nature* 489, 263-268.
- Walther, D.M., Kasturi, P., Zheng, M., Pinkert, S., Vecchi, G., Ciryam, P., Morimoto, R.I., Dobson, C.M., Vendruscolo, M., Mann, M., et al. (2015). Widespread Proteome Remodeling and Aggregation in Aging *C. elegans*. *Cell* 161, 919-932.
- 30 Wei, Y.N., Hu, H.Y., Xie, G.C., Fu, N., Ning, Z.B., Zeng, R., and Khaitovich, P. (2015). Transcript and protein expression decoupling reveals RNA binding proteins and miRNAs as potential modulators of human aging. *Genome biology* 16, 41.
- Wojcik, C., and DeMartino, G.N. (2002). Analysis of Drosophila 26 S proteasome using RNA interference. *J Biol Chem* 277, 6188-6197.
- 35 Wood, S.H., Craig, T., Li, Y., Merry, B., and de Magalhaes, J.P. (2013). Whole transcriptome sequencing of the aging rat brain reveals dynamic RNA changes in the dark matter of the genome. *Age* 35, 763-776.
- Zecca, L., Youdim, M.B., Riederer, P., Connor, J.R., and Crichton, R.R. (2004). Iron, brain ageing and neurodegenerative disorders. *Nat Rev Neurosci* 5, 863-873.
- 40 Zeier, Z., Madorsky, I., Xu, Y., Ogle, W.O., Notterpek, L., and Foster, T.C. (2011). Gene expression in the hippocampus: regionally specific effects of aging and caloric restriction. *Mechanisms of ageing and development* 132, 8-19.

Zoncu, R., Bar-Peled, L., Efeyan, A., Wang, S., Sancak, Y., and Sabatini, D.M. (2011). mTORC1 senses lysosomal amino acids through an inside-out mechanism that requires the vacuolar H(+)-ATPase. *Science* *334*, 678-683.

Supplemental Information

Materials and Methods

Figures S1-S7

Table S1

5 Tables S2-S9 (provided as separate files)

Supplemental References

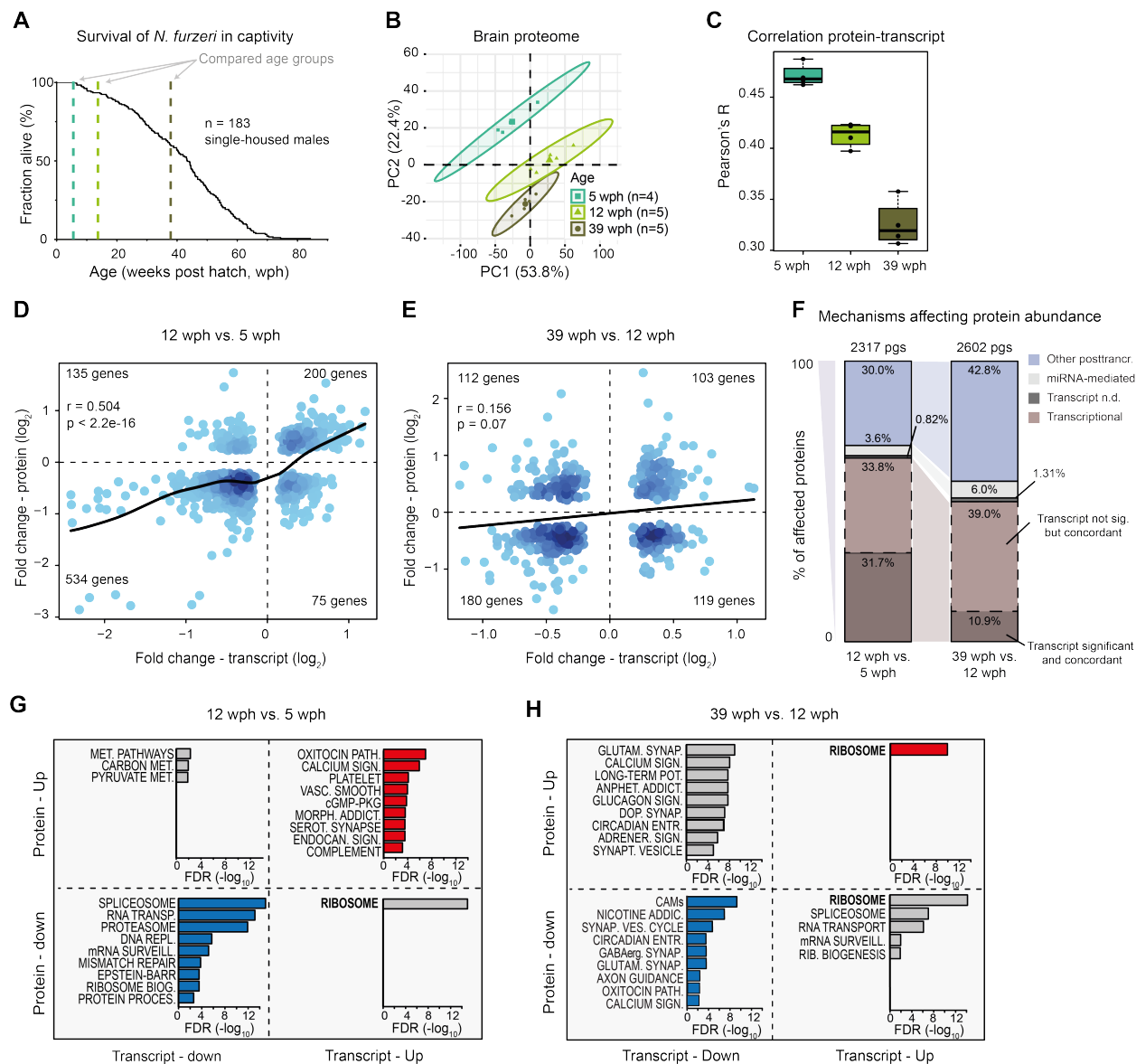


Figure 1. Transcript and protein levels become decoupled during *N. furzeri* brain aging.

(A) Survival curve of *N. furzeri* in the FLI facility. Recording of deaths starts at age of 5 wph, which corresponds to sexual maturity, and the colored dashed lines indicate the three age groups analysed in this study (5 animals/group), namely 5 weeks post hatching (wph, young, sexual maturity), 12 wph (adult) and 39 wph (old, past median lifespan) of a wild-derived strain that exhibits a median lifespan of 7-8 months. (B) Principal component analysis (PCA) of brain samples based on the abundance of all proteins identified by label-free mass spectrometry. The smaller dots represent individual samples and the larger dots the centroids of each age-matched group. Ellipses represent 95% confidence intervals. The percentage of variance explained by the first two PC axes is reported in the axis titles. (C) Global protein-transcript correlation for each sample, grouped by age. RPKM and iBAQ values were used to estimate transcript and protein levels from matched RNAseq and TMT-based proteomics data obtained from the same animal. An ANOVA test was performed to evaluate significance among the age groups (mean correlation at 5 wph: 0.48; at 12 wph: 0.43; and at 39 wph: 0.33; p = 3.05e-07). (D and E)

Scatter plot of \log_2 fold changes for genes differentially expressed both at transcript and protein levels (adj p < 0.05). The color gradients indicate gene density in the regions where individual points overlap. Numbers of genes in each quadrant and the value of Pearson's coefficient of correlation, r, are reported for each graph. Solid lines represent a spline fit (r = 0.5 for genes significantly affected at both transcript and protein levels, $p < 2.2 \times 10^{-16}$, D) (r = 0.156, p = 0.07, E). **(F)** Mechanisms affecting protein abundance during aging. Bar plots are based on all the proteins affected in either one of the age comparisons (adj p < 0.05). Proteins were divided in the following five groups: (i) proteins and transcripts with significant and consistent changes (dark brown), (ii) proteins with significant changes, and with consistent changes of the transcripts (light brown), (iii) proteins with no transcripts detected (dark gray), (iv) proteins with transcripts whose translation is potentially regulated by miRNAs (light gray), as assessed by the workflow displayed in (Figure S2C), (v) all the remaining proteins that we classified as regulated by other post-transcriptional mechanisms (violet). pgs = protein groups. **(G and H)** Bar plots representing enriched KEGG pathways among genes that showed significant changes at both transcript and protein levels in aging. Genes were grouped according to the four possible patterns of transcript and protein regulation, as visualized by their positions in the four quadrants shown in **(D)** and **(E)**, respectively. Only pathways significantly enriched (FDR < 0.05) are shown. The complete list of enriched pathways is reported in Table S5. Related to Figures S1 and S2, and Tables S1:S5.

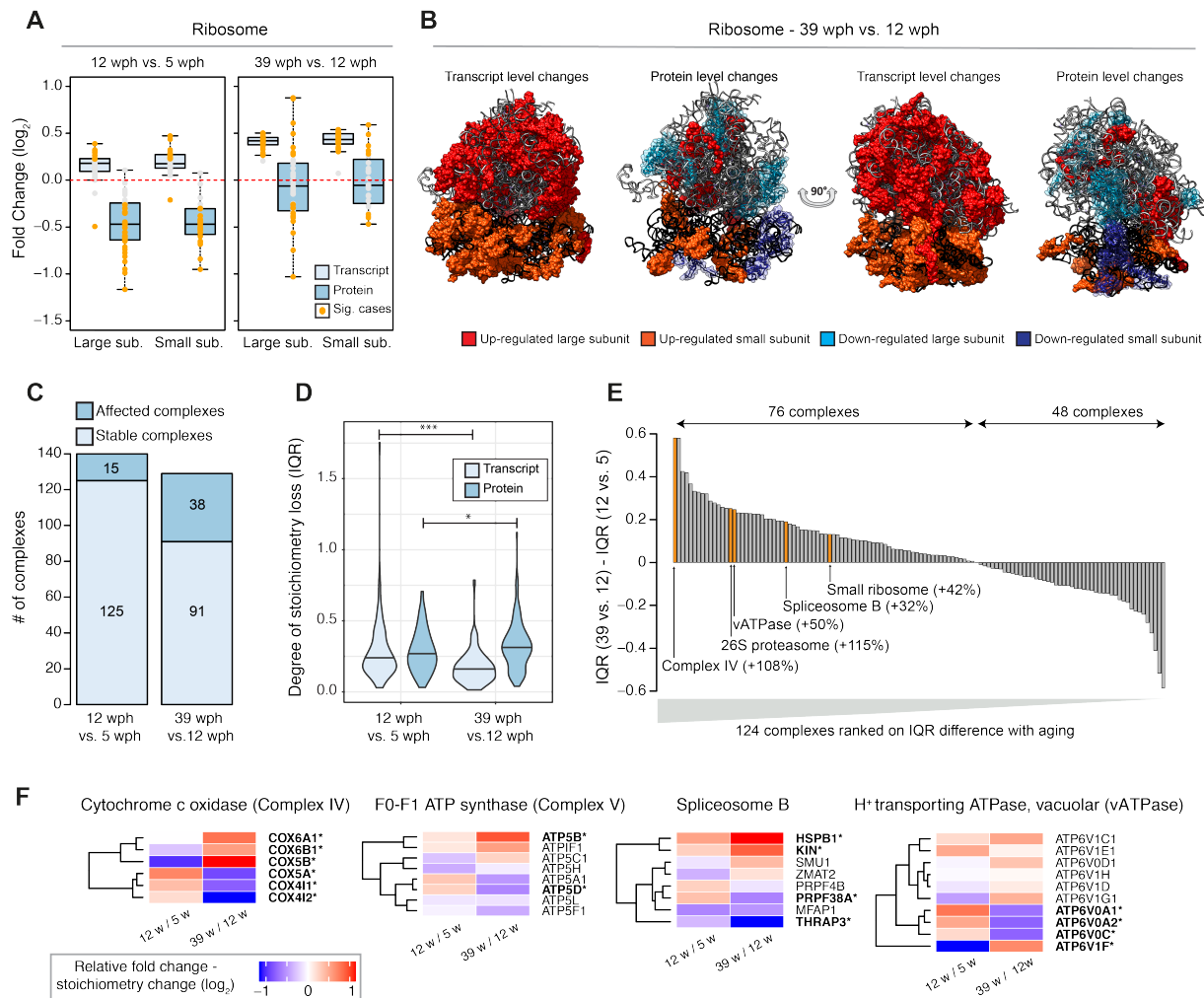


Figure 2. Global stoichiometry loss in protein complexes during aging. (A) Abundance changes of ribosomal proteins and their transcripts during aging. Cytoplasmic ribosomal proteins of large and small subunits are displayed separately and changes are shown for both the age comparisons as box plots. Transcripts are displayed as light blue and proteins as dark blue boxes. Changes of individual proteins are displayed as dots, orange dots identify significant cases (adj p < 0.05). (B) Visualization of age-related changes of proteins and transcripts projected on the 80S ribosome complex structure. Ribosomal RNA are depicted in ribbon form: 28S rRNA, 5S rRNA, 5.8S rRNA of large subunit are depicted in light gray and 18S rRNA of small subunit is depicted in black. Ribosomal proteins are depicted as molecular surfaces and shown only if significant changes in the level of corresponding mRNA or protein were detected. Affected proteins of large and small subunits are visualized in 2 different shades of red (up regulated), or blue (down regulated). For clarity, down regulated components are displayed as transparent molecular surfaces. Visualization was performed with UCSF Chimera program (version 1.12), according to Protein Data Bank archive - human 80S ribosome 3D model: 4UG0. (C) Statistics of protein complexes undergoing stoichiometry changes with aging. Only protein complexes that had at least 5 members quantified were considered for each comparison. Complexes were considered affected if at least two members showed significant stoichiometry change (adj p < 0.05 and absolute \log_2 fold change > 0.5). The complete list of stoichiometry changes is available in Table 5. (D) Violin plot showing the degree of stoichiometry loss (IQR) for transcript and protein data across different age comparisons. (E) Histogram showing the distribution of the difference in IQR between 39 vs. 12 and 12 vs. 5 for 124 complexes. (F) Phylogenetic trees for four complexes (Cytochrome c oxidase, F0-F1 ATP synthase, Spliceosome B, vATPase) comparing 12 w / 5 w and 39 w / 12 w. Colored nodes indicate relative fold change - stoichiometry change (\log_2) from -1 to 1.

5 S6. **(D)** Violin plots depicting interquartile ranges (IQRs) of individual members of protein complexes during aging. The IQR for each protein complex considered in **C** was calculated using transcript (light blue) or protein (dark blue) \log_2 fold changes between two age groups. * p < 0.05, *** p < 0.001, Wilcoxon Rank Sum test. **(E)** Bar plot showing the ranking of protein complexes based on the difference in protein level IQR for each complex between the 39 wph vs. 12 wph and 12 wph vs. 5 wph comparison. Selected complexes are highlighted and the percent 10 of IQR increase between the two age comparisons is indicated in brackets. **(F)** Heat map showing relative protein fold changes for members of selected complexes affected by aging. Names of significantly affected members in the 39 wph vs. 12 wph comparison (adj p < 0.05 and absolute \log_2 fold change > 0.5) are highlighted in bold with a star. Related to Figure S3 and Table S6.

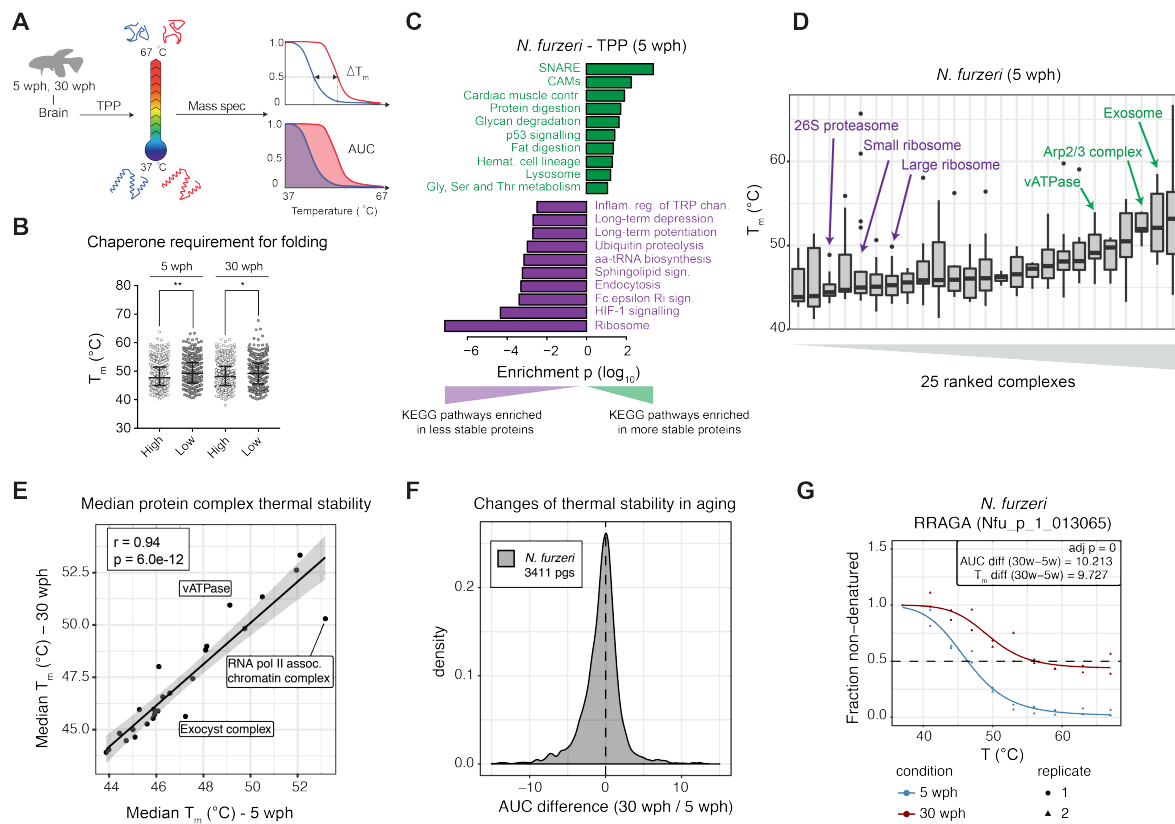


Figure 3. Changes of protein thermal stability during aging. (A) Schematic workflow of the thermal proteome profiling (TPP) procedure. The age groups compared are indicated. Melting point (T_m) and area under the curve (AUC) are illustrated.. For each age group, two independent samples were analysed. (B) Plot representing T_m distributions of proteins with high requirement of molecular chaperones for folding (top 20% of the cleverSuite scores) or self-folding (bottom 20%) in either young or aged *N. furzeri*. The bar shows the median of the dataset, and the whiskers point the interquartile range. *: $p < 0.05$, **: $p < 0.01$, ***: $p < 0.001$, Kolmogorov-Smirnov test. (C) Gene set enrichment analysis for TPP results. For each comparison, proteins were ranked according to the calculated AUC values and the enrichment of KEGG pathways calculated. Data obtained for young samples (5 wph) are shown. The 10 most significantly enriched pathways among more stable (high AUC, green) or least stable proteins (low AUC, violet) are shown ($p < 0.05$). Complete list is available in Table S7. (D) Box plot of complexes ranked according to the complex median T_m obtained from TPP experiments. Only complexes with at least 5 members quantified were considered. Selected complexes showing low or high thermal stability are highlighted in violet and green, respectively. (E) Comparison of median T_m values of protein complexes between young and old samples. The black solid line indicates the fitted linear model and the grey shade the 0.95 confidence interval of the model. Selected outlier complexes are indicated ($r=0.94$, $p=6.0e-12$). (F) Distribution of AUC differences between old and young samples in *N. furzeri*. pgs = protein groups. (G) Melting curves for RRAGA obtained by TPP from young (blue) and old (red) killifish brains. Related to Figure S4 and Table S7.

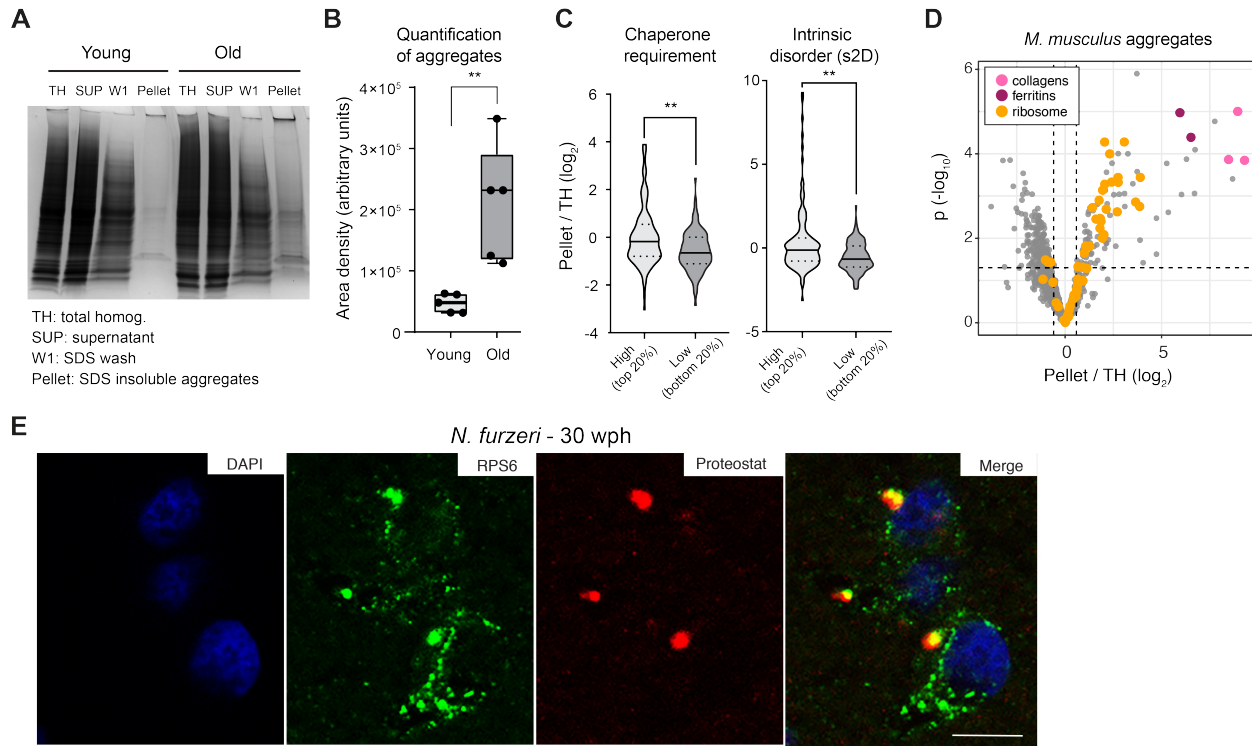


Figure 4. Aggregation of ribosomal proteins during brain aging. (A) Representative Coomassie-stained SDS-PAGE gel showing the isolation of SDS insoluble aggregates from mouse brain lysates. TH = total homogenate, SUP = supernatant, W1 = SDS-soluble fraction, Pellet = formic-acid soluble fraction (see Figure S5A). (B) Quantification of the yield of SDS-insoluble aggregates from young and old brain lysates was based on densitometry analysis of Coomassie-stained gel bands obtained from different animals, n=5 per age group (Figure S5B); ** p < 0.01, unpaired t-test. (C) Proteins enriched in aggregates show a predicted higher molecular chaperone requirement for folding (top vs. bottom 20% p=0.0055, Kolmogorov-Smirnov test), and are richer in intrinsically disordered regions (s2D-derived scores, top vs. bottom 20% p=0.0019, Kolmogorov-Smirnov test). Violin plots: the solid line shows the median, the dotted lines the interquartile ranges. The same result was obtained with cleverSuite-derived scores (top vs. bottom 20% p=0.0201, Kolmogorov-Smirnov test) (Figure S5C). (D) Volcano plot based on protein quantification by label-free mass spectrometry depicting the enrichment of specific proteins in protein aggregates. The x-axis indicates the \log_2 ratio between protein abundance in aggregates (Pellet) and starting total homogenate (TH). The horizontal dashed line indicates a p value cut-off of 0.05 and vertical lines a \log_2 fold change cut off of ± 0.5 . Selected proteins are highlighted as colored dots as indicated in the figure legend. Protein quantification was based on samples obtained from 3 independent isolations. (E) Double-labelling of telencephalic sections of *N. furzeri* with anti-RPS6 (green) as ribosomal marker and Proteostat as a marker for aggregated proteins (red). Nuclear counterstaining was performed with DAPI (blue). Scale bar = 10 μ m. Related to Figure S5 and Table S8.

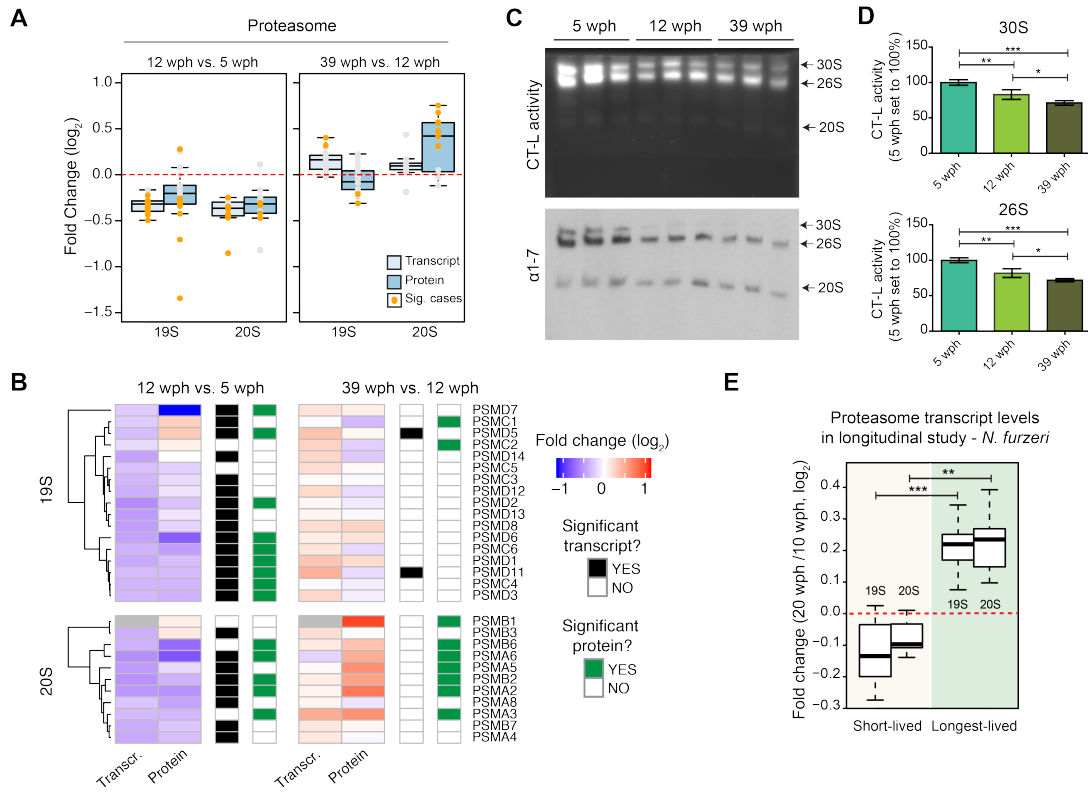


Figure 5. Reduced proteasome activity and assembly in old brains. (A) Abundance changes of proteasome proteins and their transcripts during aging. Members of the 19S and 20S complex are displayed separately and changes are shown for both the age comparisons as box plots. Transcripts are displayed as light blue and proteins as dark blue boxes. Changes of individual proteins are displayed as dots, orange dots represent significant cases (adj. $p < 0.05$). (B) Heat map showing transcript and protein fold changes for members of the 26 proteasome (19S and 12S complexes). Genes are annotated according to significance of their changes at the level of transcript (adj. $p < 0.05$: black, adj $p > 0.05$: white) or protein (adj. $p < 0.05$: green, adj. $p > 0.05$: white). (C) In-gel proteasome assay following native gel electrophoresis (top) and immunoblotting of proteasome complexes (30S, 26S and 20S) (bottom) in young (5wph), adult (12 wph) and old (39 wph) killifish brains. (D) Bar plots depicting the quantification of chymotrypsin-like (CT-L) activity from native gels calculated for doubly capped (30S) or singly capped (26S) proteasomes. $n \geq 5$ per sample group; error bars indicate standard deviation. * $p < 0.05$, ** $p < 0.01$, *** $p < 0.001$, unpaired t-test. For each sample group, the mean value of activity in young samples (5 wph) was set to 100%. (E) Downregulation of proteasome transcripts in killifish longitudinal study. Boxplot depicts average fold-changes between 10 and 20 wph for 25 fish that lived shorter than the median lifespan (short-lived) and the 25 longest-lived fish of a cohort of 152 fish (longest-lived). Statistical significance calculated by Wilcoxon Rank Sum test. Expression data were obtained from (Baumgart et al., 2016). Related to Figure S6.

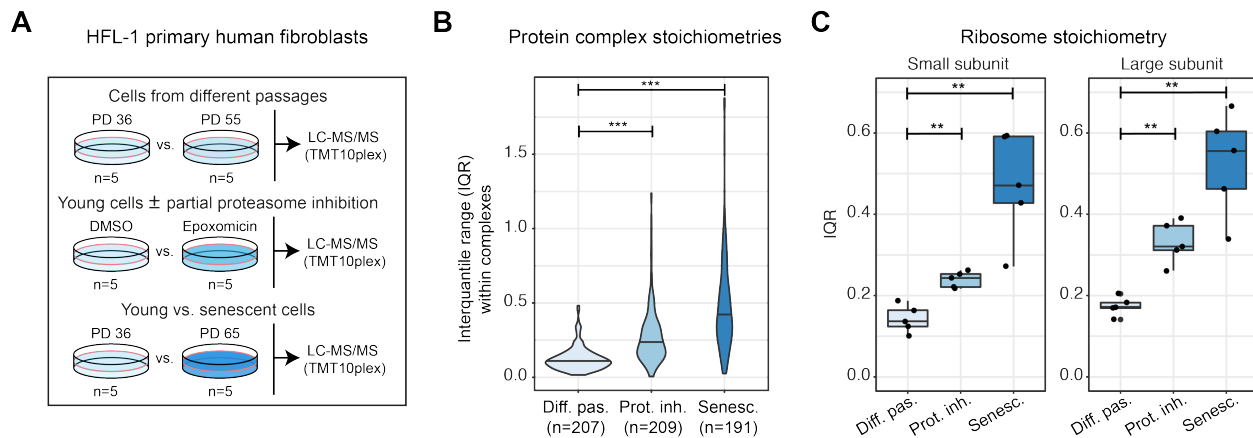


Figure 6. Partial inhibition of the proteasome is sufficient to induce loss of stoichiometry of protein complexes in primary human fibroblasts. (A) Schematic workflow depicting the proteome comparisons performed in HFL-1 fibroblasts. Three comparisons were performed: (i) fibroblasts harvested at different passages (“Diff. pas.”); (ii) fibroblast treated with the proteasome inhibitor epoxomicin for four days vs. vehicle control (“Prot. inh.”); (ii) senescent vs. young fibroblast (“Senescent”). For each comparison, five biological replicates were analysed. (B) Violin plots depicting interquartile ranges (IQRs) for protein complexes. IQRs were calculated for each complex from the protein fold changes of the respective members as in Figure 2D. The number of protein complexes analysed for each sample group is indicated. *** p < 0.001, Wilcoxon Rank Sum test. (C) Boxplots depict the IQR for large and small ribosome subunit derived from protein fold changes for each sample set. ** p < 0.01, Wilcoxon Rank Sum test. Related to Figure S7 and Table S9.